Near Net Shape Spur Gear Forging Using Concave Preform

Necip Fazil YILMAZ*, Omer EYERCIOGLU**
*Mechanical Engineering Department, University of Gaziantep, 27310, Gaziantep, Turkey,
E-mail: nfyilmaz@gantep.edu.tr
**Mechanical Engineering Department, University of Gaziantep, 27310, Gaziantep, Turkey,
E-mail: eyercioglu@gantep.edu.tr

1. Introduction

Precision forging gives shape to an initial billet, which can be used directly as a part requiring little or no further finishing. Directional alignment of the grains or fibers, which form the outline of the product during the forging process, helps improve the mechanical properties of the final forged part, imparting increased strength, ductility, and resistance to the impact and fatigue of the metal [1].

Forming gears rather than cutting them has the obvious advantage of greater utilization of raw material and high productivity. Thus, the process of forming has greater potential for large quantity batch production such as required by automotive companies and consumer goods industries. Despite these positive aspects, the economics of fully formed spur and helical gears for power transmission have not yet been proven to be acceptable and cannot be until a robust processing route is established [2].

Overall performance of the forging operation requires an understanding of not only the flow stress of the material and frictional conditions but also the mode of flow of the material. Success here depends on a thorough understanding of the metal flow during forging [3]. Although many attempts have been made to acquire the knowledge necessary to design the precision spur gear forging process, preform design and design of dies [4-9] have been used to a certain extent. Kiekbusch et al. [10] used FE analysis to calculate the combined torsional mesh stiffness of spur gears. Gear formation and failure analysis especially in gear tooth crack growth analyzed by Podrug et al [11]. They proposed that crack propagation in gear tooth is different according to loading conditions. Ohga et al. [12] analyzed the forging of spur gear with low carbon steel and low alloyed standard steel in two steps to prevent the die failure by using secondary flow, which can reduce the working pressure. Arbak et al. [13] compared the various preforms for hot forging of bearing rings by considering the coupled thermo-mechanical analysis. They concluded that there are different criteria in determining the preform shape for different parts to prolong the tool wear and to prevent the tool fracture. Cai et al. [14] discussed alternative tool designs, which may be used on a press with only one moving slide and ejection system. They examined the influence of different designs on metal flow and load requirement through experiments and finite element simulation. Chengliang et al. [15] studied on the dimensional accuracy of spur gears.

They proposed two different punch shapes to fulfill the corners because of the inhomogeneous distribution of metal blank.

The major problem associated with precision spur gear forging is related mainly to the material flow and friction between the die and billet [16-17]. Under the load, billet is bulging and getting contact with the die. The contact begins nearly midpoint of the billet height and the contact area increases with descending punch. Due to the friction effect, forging load is increasing. Although high forging loads are applied, it becomes very difficult to fill the corners of the gear die. To utilize the advantage of preforms, punch displacement and mode of metal flow should be well analyzed. Therefore, this paper proposes concave preforms to overcome insufficient corner filling problem with the application of considerably less amount of forming load. Throughout the analysis, three different types of preform geometry are searched to fulfill the die cavity of spur gear dies. One of them is the simple cylindrical form, and the other two preforms are prepared in different concavity parameters. During the analysis, correlation between the relative average load requirement and material flow behavior are captured. Deformation mode of each preform is analyzed and demonstrated with constant incremental steps. Radial flow velocity distribution is an important indicator to be evaluated for metal flow and, thus, forming load. To analyze the velocity distribution, four different representative nodes are investigated. According to the concavity, a feasible preform is suggested for which the total forming load could be reduced by 34%. The predicted forging loads obtained by finite element methods are shown to approximate the experimental results at final filling up stage.

2. Die filling and problem definition

Because precision spur gear forging dies obtain very high radial pressure during the process, it considerably deforms in the radial direction. This radial deformation of the die becomes an important factor influencing the dimensional accuracy of the product. To obtain the product with highly accurate dimension and within relatively less amount of load, it is therefore essential to acquire some information on the die filling and load stroke diagram. Hollow cylindrical billets often are used to forge net-shape axisymmetric and hollow parts such as gears used in power transmission systems. The precision shape can be formed with parallel bores by using completely closed dies with mandrels. Various tool set designs are possible for finishing the forging of gears in completely closed cavity dies [18]. An important feature of completely closed forging dies is how the workpiece is deformed to fill the die cavity. For the simple shapes, the deformation mode can be identified by the order of filling of top and bottom corners of the cavity. Fig. 1

shows a workpiece enclosed in die cavity with the punch and ejector [19].
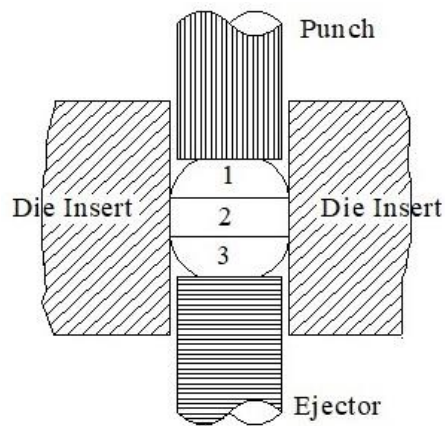

Fig. 1 Deformation mode of billet: *1* - upper section, *2* -mid-section, *3* - bottom section

The workpiece height initially gets smaller until the outermost side of the workpiece touches the die wall while the punch is moving downward. Barrelling almost start at the middle of the workpiece. Therefore, friction between the die wall and the workpiece plays an important role for the required forging load. After that point, the volume of the part and contact area, shown by number *2* in Fig. 1, starts to increase because of the increment in its height. This means that more forging load is required. In the final stage, the corners of the product remain a little bit circular.

The dimensions of the forged tooth form depend not only on the expansion because of the elevated temperatures of the billet and the tools but also on the elastic expansion of the forging tools because of the radial pressure, which is related to the forging load required to complete the forged shape. In gear forging, the mid-section of the gear teeth fills in advance of the top and bottom faces. It is in the last stages of forging that the top and bottom corners of the teeth are filled, and thus, this filling requires high forging force. A significant increase in load arises when the workpiece reaches the die. Near to the end of the process, forging load increases sharply, and approximately 25% of the total forming energy is consumed in this final stage [13].

Z.M. Hu and T.A. Dean [20] states that in the final punch movement of 0.3 mm, 1.2% of the billet deformation to fill the corner was accompanied by a load increase of nearly 50%. Easing flow into the corners by die design techniques or designing gears, which do not have sharp corners can dramatically reduce forging load requirements and tool stresses. The benefit will be less distortion, better dimensional accuracy, and longer tool life. Another aspect of precision spur gear forging is extrusion of workpiece material through the punch clearance when the bottom of the die corner is filled.

This fin formation is undesirable before complete die filling because when the fin starts, it continues to form at an approximately constant extrusion load. Therefore, the pressure in the die cavity cannot be increased to fill the unfilled areas, and also, the dimensional accuracy cannot be obtained because of material loss in the fin formation. A typical fin formation is shown in Fig. 2**.**

Fig. 2 Fin formation

3. Formation of tooth form and process simulation

Three-dimensional finite element model of a gear forging process has been created to decide the feasible preform geometry. During the modelling, three different types of preform were analysed by providing the volume constancy. The commonly used preform for the forging of a spur gear is a hollow cylindrical billet with its outer diameter close to the root diameter of the gear. Thus, in the first case, the top radius and the bottom radius of the cylindrical billet were kept constant with no concavity on the cylindrical surface. In the second case, the top and bottom radii were kept constant, but concavity has formed on the cylindrical surface. In the third case, both concavity on the cylindrical surface and top radius were altered. Bottom radius was determined as the root radius of the gear for all cases. Many different alternatives were simulated, but for the sake of brevity, 26 cases of gear forging were realized as shown in Table 1. Schematic drawing of preform types are shown in Fig. 3.

Table 1

Preform geometry alternatives

	Top Radius (R_{top}) (mm)	Bottom Radius (R_{bottom}) (mm)	Concavity (R_c) (mm)
Case 1	32.5	32.5	No
Case 2	32.5	32.5	120, 130, 140, 150, 160
Case 3	28,29,30, 31	32.5	120, 130, 140, 150, 160

All numerical simulations have been performed for AISI-4340 hot forming steel. AISI 4340 is a heat-treatable, low-alloy steel containing nickel, chromium, and molybdenum. It is known for its toughness and capability of developing high strength in the heat-treated condition while retaining good fatigue strength. Process parameters are presented in Table 2.

Table 2

Process parameters

Billet material	AISI 4340
Module	3
Number of teeth	24
Pressure angle	20
Initial billet temperature	900 ^{0}C
Surrounding temperature	20 ^{0}C

Water-based graphite was used as tools and workpiece lubricants, and a frictional factor of 0.25 was used in

FEM simulations. Also, heat transfer was accounted by coupled thermomechanical analysis between the tools and workpiece.

In the analysis, to decrease computer CPU time, rigid model was assumed for tool material, and only one half of the gear tooth portion was used because of its symmetry. Schematic representation of analysis and the CAD drawing is shown in Fig. 4.
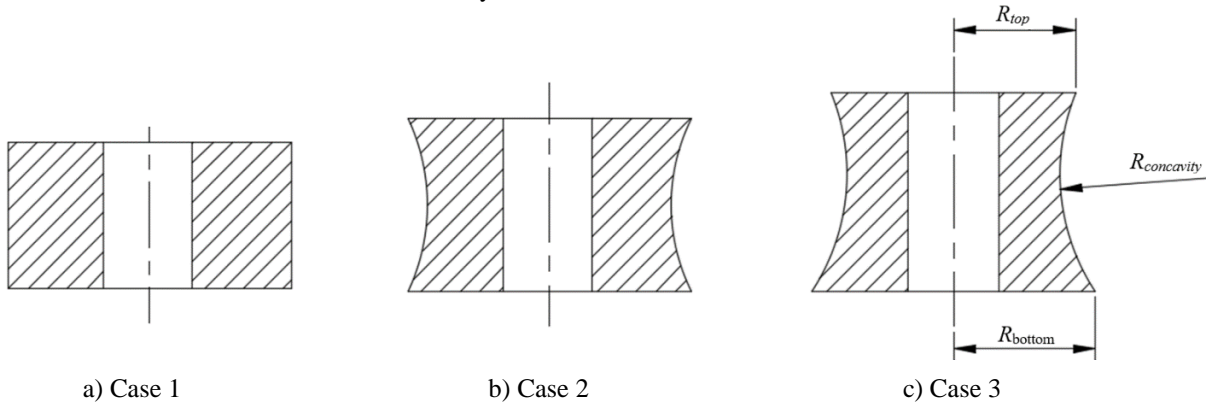

a) Case 1   b) Case 2   c) Case 3

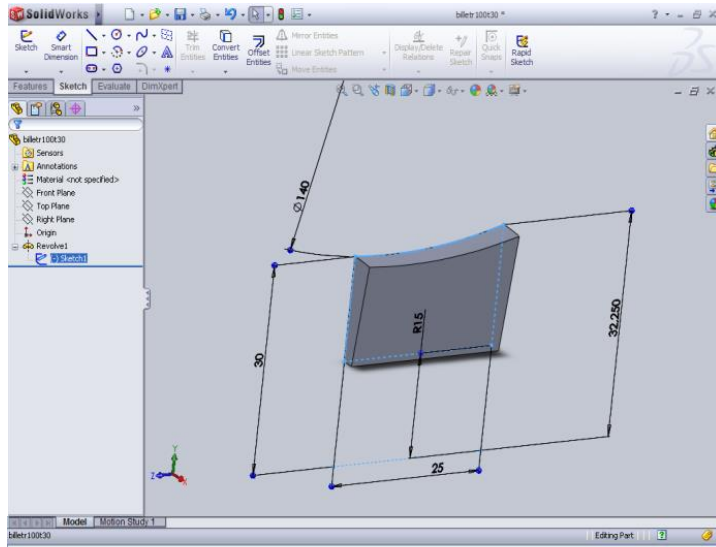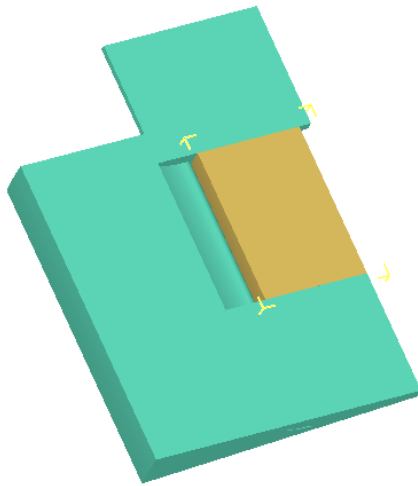Fig. 3 Preform forge geometries studied in this work

Fig. 4 Die and workpiece representation

4. Results and discussion

Velocity distributions and displacement diagrams of four different nodes for each case were considered to discuss the influences of preform geometry. Forging loads were then carefully examined because excessive load causes the die failure, whereas less amount of load causes insufficient corner filling.

4.1. Velocity distributions

Radial flow velocity distributions have vital importance to understand the metal deformation because the cylindrical gear blank is forced to flow radially. The velocity distribution, which predicts the lowest work rate, is the best approximation of the actual velocity distribution. This principle states that the material should always flow in the path of least resistance. The lowest work rate principle for rigid plastic materials can be expressed as shown in Eq. (1).

$$\pi = \int_v \overline{\sigma}\, \dot{\overline{\varepsilon}}\, dV - \int_{S_F} F_i - u_i DS. \qquad (1)$$

The manner in which this equation is solved for the velocities can be seen in Eq. (2). This variational approach requires admissible velocities (u_i).The velocities are solved by solving for when the variation in the functional is stationary. Because the total solution should be zero, the solution will tend to maintain a low volumetric strain rate to keep this integral value low.

$$\delta\pi = \int_v \overline{\sigma}\, \delta\dot{\overline{\varepsilon}}\, dV + K\int_v \dot{\varepsilon}_v\, \delta\dot{\varepsilon}_v\, dV - \int_{S_F} F_i \delta u_i DS = 0, \qquad (2)$$

where: $\overline{\sigma}$ is the effective stress, $\dot{\overline{\varepsilon}}$ is the effective strain rate, F_i represents surface tractions, $\delta\dot{\overline{\varepsilon}}$ and $\delta\dot{\varepsilon}_v$ are variations in strain rate derived from δu_i and K is a penalty constant [21]. The solution for Equations 1 and 2 are the velocities at each node, which are shown as vector arrows in Fig. 5.

The velocity of the top set of nodes is determined by the downward speed of the die as well as the friction model between the billet and the gear die. As it is depicted in Fig. 6, the boundary conditions of [AB] on the left side of

the die are specified as a centerline condition, meaning that the nodes are not allowed to move either right or left. The bottom nodes also have a symmetry condition, meaning that they are not allowed to move up or down. These three boundary conditions allow the mesh to behave as the actual part.
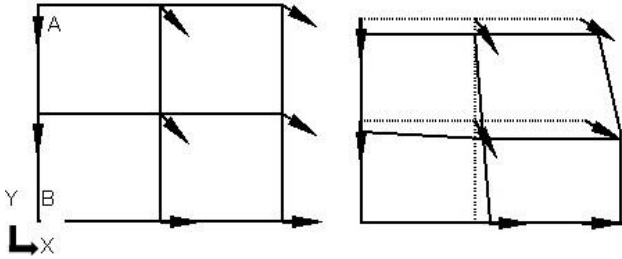

Fig. 5 Nodal velocity vector
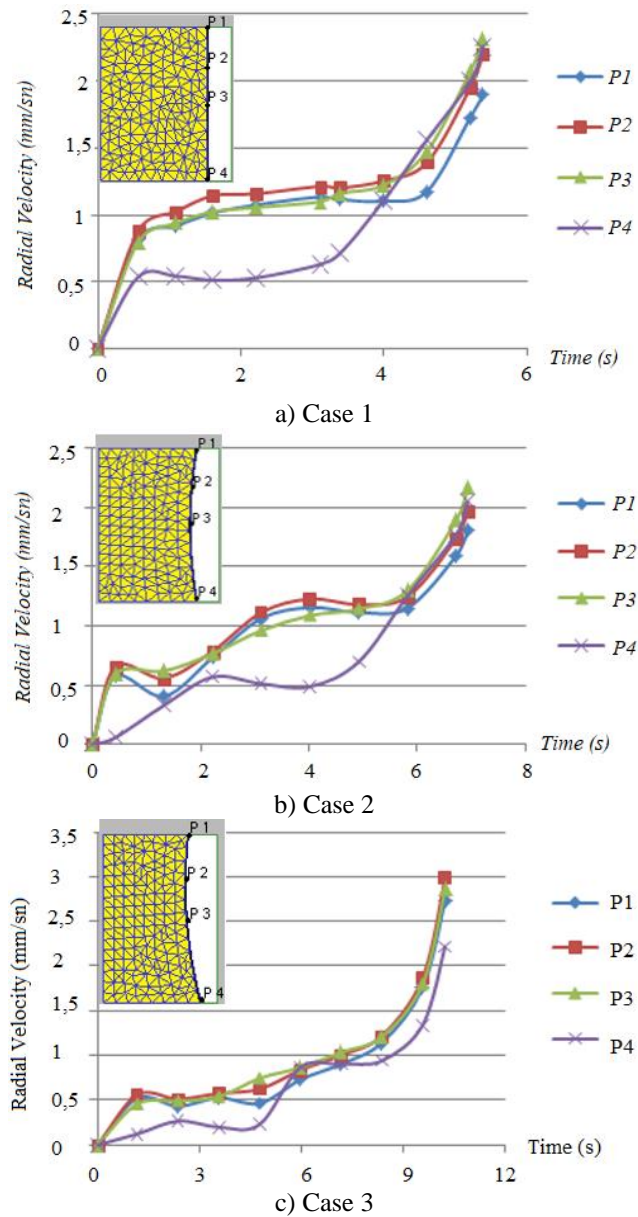

a) Case 1

b) Case 2

c) Case 3

Fig. 6 Radial velocity distributions of nodes P1, P2, P3, P4 for all cases

If the nodal velocities change direction or magnitude over very small periods, a small time step size is required to correctly predict this behavior.

$$x(t + \Delta t) = x(t) + v_x \Delta t.$$
$$y(t + \Delta t) = y(t) + v_y \Delta t. \tag{3}$$

The situation is now addressed to different concave preforms over a discrete set of points. Figs. 6 a, b and c show radial velocity (x direction) distributions for cases 1, 2, and 3, respectively. It is evident that the radial flow velocity of point $P2$ for case1 is faster than the other points. Because of the metal flow transfer from top to bottom, point $P4$ is moving rather slowly, and thus, there is a velocity difference between points $P1$ and $P4$ during deformation process. This is clearly showing the reason why filling of die corners is the main problem. As shown in Figs. 6 b and c, the radial flow velocity of $P1$, $P2$, and $P3$ for cases 2 and 3 are almost the same at initial stages. After certain stages, the center part of the billet is moving faster. Because of the concavity of the billet, $P1$, $P2$, and $P3$ are touching the die surface almost at the same time, whereas the bottom corner has not been reached by the die corner. Compared with case 1, forging load is relatively reduced, as seen in Table 3. Compared with the first two cases, Fig. 6 c shows that the points coincide each other and touch the die surface almost at the same time. Because the contact area and friction are reduced, total forging load is considerably reduced, and the corners are completely filled.

4.2. Displacement diagrams

Using a concave circular surface in the die entry moves the neutral plane toward the part and reduces the forging load. A good picture of the degree of deformation that takes place in different regions of a cylinder specimen upon axial compression may be obtained by drawing an isostrain contour map. The effective strain distribution presented in Fig. 7 shows that the center part of the billet belongs to large deformation area, and this area reaches the yield limit first. It should be noted that the effective strain is about 7 times greater in the vicinity of the corners of the specimen than at the center of its ends. In general, the average forming load depends on the inherent flow stress of the billet, the strain pattern determined by the geometry of the billet and effect of friction at the die material interface. These conditions can be categorized in terms of the k/μ ratio, where $k = 1/\sqrt{3} = 0.577$ for the von Mises criterion, and μ is the coefficient of friction. According to von Mises criterion, τ_0 is related to the flow stress in compression by $\tau_0 = \overline{\sigma} / \sqrt{3}$. The following axisymmetric equation [22] for the pressure distribution at the platen cylinder interface for which sliding friction occurs over the entire surface is obtained:

$$\frac{P}{\overline{\sigma}} = e^{2\mu/h(d/2-r)}, \tag{4}$$

where: P is the normal interfacial pressure, d is the diameter of the billet, and h is the height of the billet. The analytical expression for the critical radius r_c can be found by equating the frictional drag μp for sliding friction to that for sticking friction $\dfrac{\overline{\sigma}}{\sqrt{3}}$ as follows:
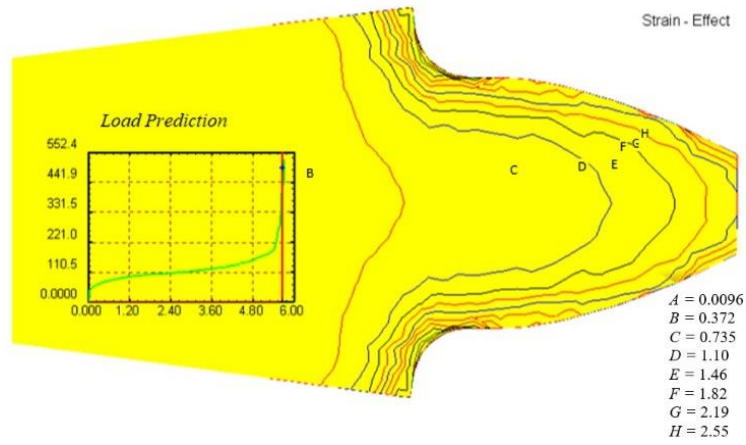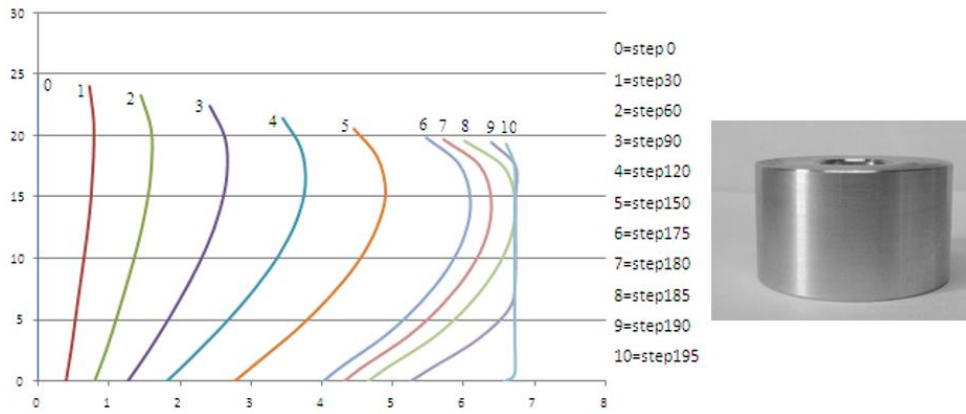
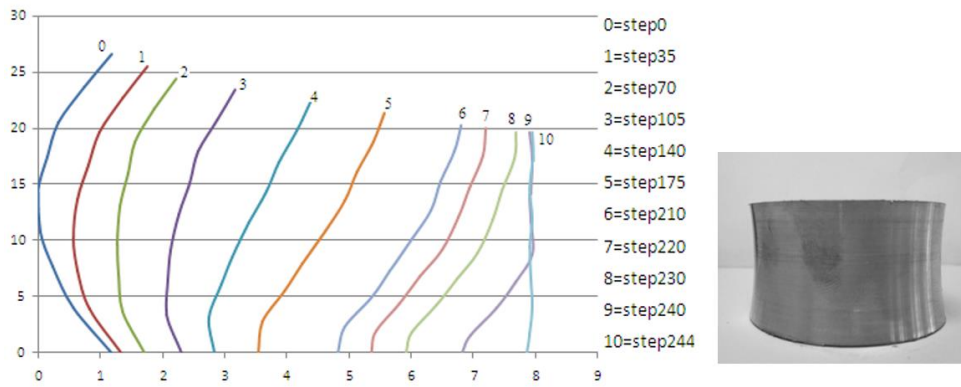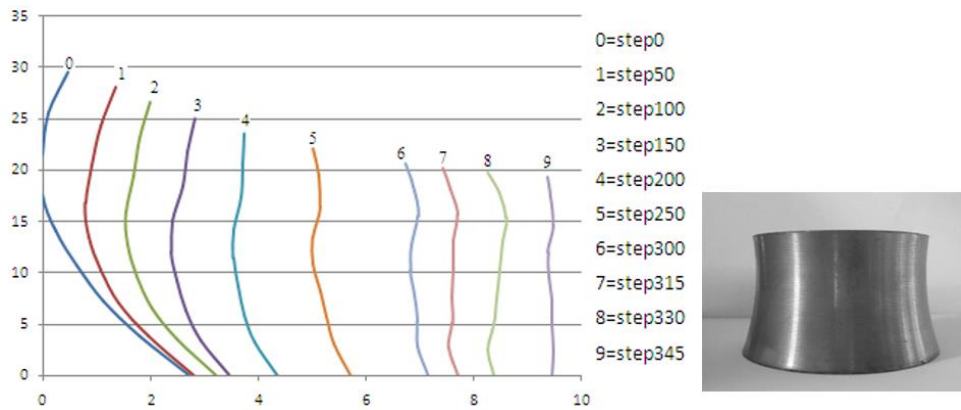Fig. 7 Effective strain distribution

a) Case 1

b) Case 2

c) Case 3

Fig. 8 Displacement diagrams for different preforms

$$\mu\,p = \frac{\overline{\sigma}}{\sqrt{3}}. \tag{5}$$

By substituting p into Eq. (4) and taking the neutral logs of both sides:

$$r_c = \frac{d}{2} - \frac{h}{2\mu} ln\left(\frac{1}{\mu\sqrt{3}}\right) \tag{6}$$

This r_c value defines the radial distance from the center to any point on the face of the billet. To realize the deformation area, nodal displacement of nodes was recorded by point tracking facility of DEFORM 3D. In the following Fig. 8, point tracking is used to show how material moves and plots of strain distributions at these points.

In the first case, simple hollow cylindrical billet is forged. Displacement diagram of case 1 is shown step by step in Fig. 8, a. It is seen that the mid-section of the workpiece grows faster than the top and bottom corners because of the frictional force on the top and bottom faces of the workpiece. Because the metal flow is transferred from top to bottom along the billet, the top corner is filling first.

Deformation process of the second preform alternative is shown in Fig. 8, b. In this alternative, a certain concavity is given to the preform geometry. During gear forging, the mid-section of the tooth gets contact with the die surface faster than the top and bottom. The frictional resistance from the die surface acts differently according to punch movement. During the punch movement, the frictional force opposes the metal flow downward, and the top region fills more rapidly. Thus, the upper face of the workpiece is formed prior to the middle and bottom regions. In the third alternative, because the top and mid surfaces of the billet are moving faster, the top surface radius was reduced relative to the bottom radius of the gear (Fig. 8, c). The bottom surface remains at the root diameter of the gear blank. In this case, the top and bottom corners and the mid-section of the toothed gear get contact with the die surface in good accordance. Also, corners are completely filled in a reasonable step with considerably less amount of forging load.

4.3. Forming load simulations

Load values for different cases of gear forging simulations are presented in Table 3. It is noticed that there is a dramatic change in forging load. In case 1, minimum load to fill the spur gear die cavity is 494.2 tons, whereas in case 3, it is 324.9 tons. This means that the total forging load is approximately saved by 34% through the use of concave preform.

Table 3

Forging load results of FEM simulations

		$R_{(top)}$ (mm)	$R_{(bottom)}$ (mm)	$R_{(concavity)}$ (mm)	Load (ton)
1	**Case 1**	**32.25**	**32.25**	**-**	**494.2**
2		32.25	32.25	120	396.3
3		32.25	32.25	130	383.6
4	**Case 2**	32.25	32.25	140	393.9
5		**32.25**	**32.25**	**150**	**331.3**
6		32.25	32.25	160	445.3
7		28	32.25	120	436.5
8		28	32.25	130	402.2
9		28	32.25	140	390.9
10		**28**	**32.25**	**150**	**324.9**
11		28	32.25	160	448.7
12		29	32.25	120	417.8
13		29	32.25	130	423.7
14		29	32.25	140	439.9
15		29	32.25	150	415.9
16		29	32.25	160	450.4
17	**Case 3**	30	32.25	120	361.1
18		30	32.25	130	412.9
19		30	32.25	140	433.5
20		30	32.25	150	447.7
21		30	32.25	160	389.9
22		31	32.25	120	425.7
23		31	32.25	130	338.1
24		31	32.25	140	417.4
25		31	32.25	150	434.0
26		31	32.25	160	439.4

Because of symmetry, a portion corresponding to only one half of the gear teeth was used for analysis. Load stroke diagrams of these three alternative gear forging cases are shown in Fig. 9. Forging load to fulfill the die cavity for cases 2 and 3 is considerably reduced compared with case1.

Forging loads are carefully examined because excessive load will cause the die to expand, impairing the accuracy of the forged parts and reducing the die life. On the other hand, less amount of load will cause the insufficient corner filling.

Table 4, 5 and 6 show the forming stages of FE simulation of three different concave preform.
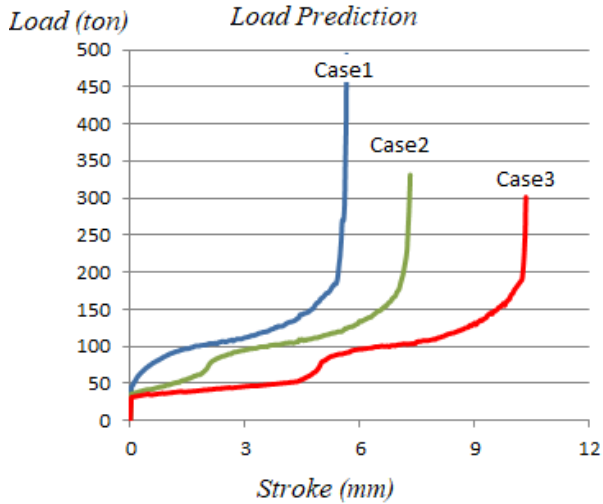

Fig. 9 Load-stroke diagrams

It is very apparent that the tooth formation of concave preforms completely filled the die with less amount of load. In these tables, PD denotes punch displacement and S is the percentage of total stroke that is calculated as:

$$S(\%) = \frac{PD}{H_i - H_f} 100, \qquad (7)$$

where: H_i and H_f are the initial and final height of the billet, respectively.

Due to volume constancy of all billets, initial heights and thus the punch displacement are different. In Fig. 10 the variation of forging loads with respect to stroke percentage is shown to compare all three cases independent from the punch displacement. The analysis and geometric models were generated using DEFORM 3D. In the early stages of gear forging, billet behaves as open die forging. Thus, the material in the middle section flows faster than the material in the top and bottom regions because of the friction force on the punch and the counterpart. As it is also clear from Fig. 10 that the inclination in the forming load up to 95% of the punch stroke is almost the same, whereas the main increment in the forming load is recorded at the last 2% of the punch stroke. Thus, the die cavity is completely filled at the end of the process, leaving no free surfaces at the corner.

Table 4

Gear tooth simulation for CASE 1

Height	24.34 mm	21.95 mm	21.13 mm	20.18 mm	20.08 mm	20.00 mm
PD	1.31 mm	3.65 mm	4.52 mm	5.47 mm	5.57 mm	5.65 mm
S (%)	25	65	80	95	98	100
Load (ton)	94.92	122.32	143.85	186.42	269.11	494.20

Table 5

Gear tooth simulation for CASE 2

Height	25.49 mm	22.55 mm	21.47 mm	20.36 mm	20.15 mm	20.00 mm
PD	1.83 mm	4.77 mm	5.85 mm	6.96 mm	7.17 mm	7.32 mm
S (%)	25	65	80	95	98	100
Load (ton)	62.1	111	127.7	172.7	209.9	331.3

Gear tooth simulation for CASE 3

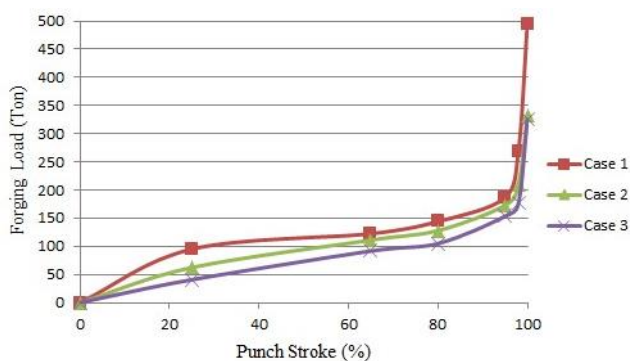|						
Height	30.66 mm	24.96 mm	22.83 mm	20.68 mm	20.26 mm	20.00 mm
PD	3.57 mm	9.27 mm	11.4 mm	13.55 mm	13.97 mm	14.23 mm
S(%)	25	65	80	95	98	100
Load(ton)	40.56	91.49	104.7	153.14	176.14	324.9

Fig. 10 Forging load variation with respect to punch stroke

5. Experimental study

The preform type commonly used in traditional spur gear forging is to use hollow cylindrical billet with its external diameter equal to the almost gear tooth root diameter. In this study, contact time between the die and the workpiece is reduced using concave preform, and therefore, forging load is considerably reduced. Fig. 11 shows the die used in the experiment and the forged gear obtained from concave preform.

Fig. 11 Die and forged gear

Schematic representation of die configuration is shown in Fig. 12. The right-hand side is the arrangement of die elements before the deformation, whereas the left side is after deformation. In this configuration, the punch is shown as a single unit, and the detail of the punch is not given for the sake of clarity. The punch forms the top surface of a cavity and is attached to the moving ram of a forging machine.

The ejector is used to remove the product from the die without deforming them and for easy removal of scale and lubricant deposits.

Die insert forms the inner side of the die (die cavity, toothed die). Because die insert is subjected to forging load, friction load, and temperature, its material must be chosen so that it resists all required conditions. To increase the resistance against internal pressure, it is usual to make an insert shrink fitted into one or more shrink rings. The compressive stress imposed by the shrink ring has cumulative effect on the bore of the die insert. Therefore, resultant tensile stress on the bore caused by the forging loads transmitted through the forging part can be substantially reduced.
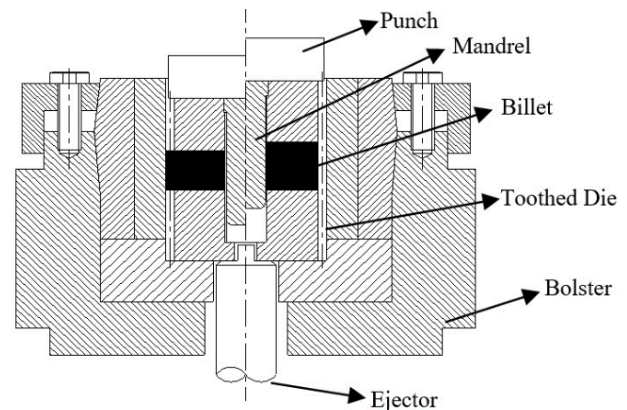

Fig. 12 Spur gear forging tool design

The preforms were heated to 1000°C in 10 minutes in order to minimize pre-forging scale formation and decarburization. They were taken from the furnace, momentarily immersed in water to break off scale, quickly placed in die and forged at 900°C. During forging trials, the 24-teeth gear with a height of 20 mm and a module of 3 mm is forged. Forging loads versus stroke acting on the punch were recorded. Fig. 13 shows punch stroke percentage versus forming load. It is seen that there is high correlation between the experimental results and the FE verification of proposed concave preform. All forging experiments were carried out under the same conditions as used for the finite element simulation.
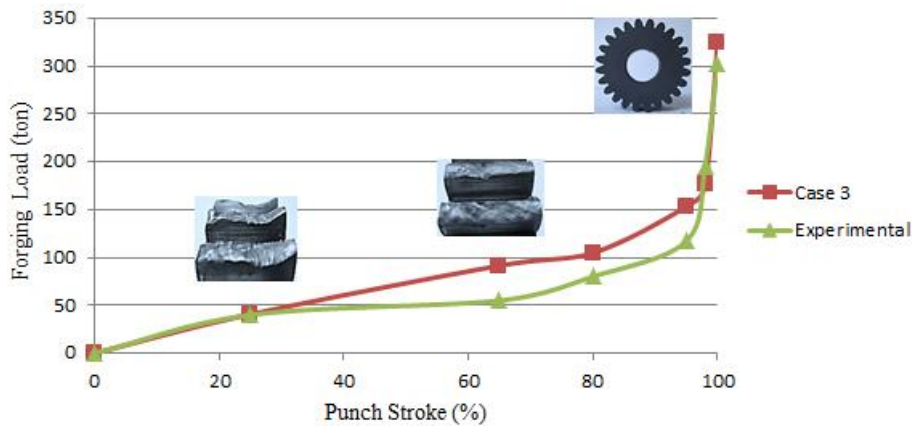
Fig. 13 Verification of FE prediction and experimental result

6. Conclusions

The total forging load consist mainly of deformation load and friction load. The frictional force between the die and the workpiece interface plays an important role in die filling and total forging load. Cylindrical flat (no concavity) billets are generally used in precision spur gear forging. The mode of metal flow is very close to open die forging if cylindrical flat sided (no concavity) billets are used. Due to barreling effect, mid-section of the billet touches to the die wall prior to its top and bottom corners. Due to friction effect and longer contact time between the billet and thee die corner filling requires very high loads. It is noticed that final punch movement of 0.26 mm and 2% of the billet deformation to fill the corner was accompanied by a load increase of nearly 45%.

This study presented a new biller geometry named as concave preform to overcome this problem. After various preform concavities were analyzed, a particular concave geometry was prepared for the selected spur gear (3 mm made, 24 teeth AISI 4340 steel) forging. The results of FE simulations and experimental studies were shown that the forging load was reduced 34% and better corner filling by using the concave pre-form compared to simple cylindrical (no concave) billet.

By the investigation of velocity distributions of the cylindrical billet, the inhomogeneous distribution of radial velocity of the billet is the main cause of insufficient corner filling. It was concluded that the lowest work rate principle is the best approximation of the actual velocity distribution.

Acknowledgment

References

1. **Eyercioglu, O.; Walton, D.; Dean, T.A.** 1997. Comparative bending fatigue strength of precision forged spur gears, Proceedings of IMechE Part-C Journal of Mechanical Engineering Science 21: 4: 293-299. https://doi.org/10.1243/0954406971522051.

2. **Dean, T.A.** 2000. The Net-shape forming of spur gears, Materials and Design 21: 271-278. https://doi.org/10.1016/S0261-3069(99)00074-6.

3. **Naunit, R.C.; Yohng, J.K.** 2001. Near net shape forging of a crown gear: Some experimental results and analysis, International Journal of Machine Tools & Manufacture 41: 325-346. https://doi.org/10.1016/S0890-6955(00)00083-3.

4. **Qingbin, L.; Shichun, W.; Sheng, S.** 1998. Preform design in axisymmetric forging by a new FEM-UBET method, Journal of Materials Processing Technology 74: 218-222. https://doi.org/10.1016/S0924-0136(97)00271-9.

5. **Yilmaz, N.F.; Eyercioglu, O.** 2009 An integrated computer aided decision support system for die stresses and dimensional accuracy of precision forging dies, International Journal of Advanced Manufacturing Technology 40: 9-10: 875-886 https://doi.org/10.1007/s00170-008-1402-z.

6. **Yilmaz, N.F.; Eyercioglu, O.** 2008 Knowledge based reverse engineering tool for near net shape axisymmetric forging die design, Mechanika 5: 65-73.

7. **Yilmaz, N.F.; Eyercioglu, O.** 2003 Application of UBET in the prediction of forging load for axisymmetric forging, Int J Adv Manuf Syst 6: 1-11.

8. **Eyercioglu, O.; Kutuk, M.A.; Yilmaz, N.F.** 2009. Shrink fit design for precision gear forging dies, Journal of Materials Processing Technology 209: 2186-2194. https://doi.org/10.1016/j.jmatprotec.2008.05.016.

9. **Jin, J.; Xia, J.; Wang, X.; Hu, G.; Liu, H.** 2009. Die design for cold precision forging of bevel gear based on finite element method, Journal of Central South University of Technology 16: 546-551. https://doi.org/10.1007/s11771-009-0091-6.

10. **Kiekbusch, T.; Sappok, D.; Sauer, B.; Howard, I.** 2011. Calculation of the combined torsional mesh stiffness of spur gears with two- and three-dimensional parametrical FE models, Strojniski vestnik - Journal of Mechanical Engineering 57, 11: 810-818. http://dx.doi.org/10.5545/sv-jme.2010.248.

11. **Podrug, S.; Glodez, S.; Jelaska, D.** 2011.Numerical modelling of crack growth in a gear tooth root, Strojniski vestnik - Journal of Mechanical Engineering 57, 7-8: 579-586. http://dx.doi.org/10.5545/sv-jme.2009.127.

12. **Ohga, K.; Kondo, K.; Jitsunari, T.** 1985. Research on precision die forging utilizing divided flow, Bulletin of the Japan Society of Mechanical Engineers 28: 2451-2459.

https://doi.org/10.1299/jsme1958.28.2451.

13. **Arbak, M.; Tekkaya, A.E.; Ozhan, F.** 2005. Comparison of various preforms for hot forging of bearing rings, Journal of Materials Processing Technology 169: 72-82.
https://doi.org/10.1016/j.jmatprotec.2004.11.020.

14. **Cai, J.; Dean, T.A.; Hu, M.** 2004. Alternative die designs in net-shape forging of gears, Journal of Materials Processing Technology 150: 48-55.
https://doi.org/10.1016/j.jmatprotec.2004.01.019.

15. **Chengliang, H.; Kesheng, W.; Quankun, L.** 2007. Study on new technological scheme for cold forging of spur gears, Journal of Materials Processing Technology 187-188: 600-603.
https://doi.org/10.1016/j.jmatprotec.2006.11.037.

16. **Long, L.; Feng, X.; Tao, J.; Qi, Z.; Sungki, L.** 2010. Characteristic evaluation of friction and wear in the C-N and TiN coated gear, Int Journal of Precision Engineering and Manufacturing 11: 107-111.
https://doi.org/10.1007/s12541-010-0013-4.

17. **Eyercioglu, O.; Dean, T.A.; Walton, D.** 1994. Dimensional accuracy of hot precision forged spur gears, Proceedings of the 1994 International Gearing Conference, Newcastle upon Tyne 285-290.

18. **Tuncer, C.; Dean, T.A.** 1987. Design alternatives for precision forging hollow parts, International Journal of Machine Tools and Manufacture 27: 65-76.
https://doi.org/10.1016/S0890-6955(87)80040-8.

19. **Vidal-Salle, E.; Boutabba, S.; Cui, Y.; Boyer, J.C.** 2008. An improved plastic wave friction model for rough contact in axisymmetric modelling of bulk forming processes, International Journal of Material Forming 1: 1263-1266.
https://doi.org/10.1007/s12289-008-0132-y.

20. **Hu, Z.M.; Dean, T.A.** 2000. Some aspects of net shape forging of gears, Proceedings of the Second International Seminar on Precision Forging 127-132.

21. **Kobayashi, S.; Oh, S.I.; Altan, T.** 1989. Metalforming and the finite-element method, 1st ed. Oxford University Press.

22. **Mielnik, E.M.** 1991. Metalworking Science and Engineering, 1st ed. McGraw-Hill.

N. F. Yilmaz, O. Eyercioglu

NEAR NET SHAPE SPUR GEAR FORGING USING CONCAVE PREFORM

S u m m a r y

The objective of this paper is to determine the feasible preform forge geometry for spur gear blank to reduce the forging load requirement. This paper discusses the effects of different preform geometries on the forming behavior of precision forged gear wheel geometry. It is identified that material flow and friction between die and billet are encountered as the major problem in precision forging. Radial flow velocity distributions and displacement diagrams of preform types in accordance with the forming stages were put into perspective. The analyzed preforms were evaluated in terms of forging load versus punch displacement diagrams. The effect of concave preforms on the material flow and the resulting manufacturing quality by finite element simulation in comparison with practical forging tests were analyzed to ensure a proper die filling and load requirements. Finally, a concave preform is proposed for which the forming load could be reduced by 34%.

Key words: spur gear, precision forging, preform design, concave preform.